

ON THE INTERPLAY OF FERMIONS AND MONOPOLES IN COMPACT QED₃

SIMON HANDS^a, JOHN B. KOGUT^b and BIAGIO LUCINI^{a,c}

^a *Department of Physics, University of Wales Swansea, Singleton Park, Swansea SA2 8PP, U.K.*

^b *Department of Energy, Division of High Energy Physics, 1000 Independence Avenue SW,
Washington D.C. 20585-1290*

and

*Department of Physics, University of Maryland, 82 Regents Drive, College Park, MD20742,
U.S.A.*

^c *Institute for Theoretical Physics, ETH Zürich, CH-8093 Zürich, Switzerland.*

The infra-red properties of three-dimensional abelian lattice gauge theory are known to be governed by a neutral plasma of magnetic monopole excitations. We address the fate of these monopoles in the presence of light dynamical fermions, using a lattice formulation of compact QED₃ with $N_f = 4$ fermion flavors supplemented by a four-fermi contact term permitting numerical Monte Carlo simulations in the chiral limit. Our data hint at a restoration of chiral symmetry above a critical value of the (inverse) coupling β . By performing simulations in a sector of non-vanishing magnetic charge, we are able to study the response of the theory to an external magnetic test charge. Our results suggest that the monopole plasma persists even once chiral symmetry is restored, and hence survives the continuum limit.

1 Introduction

Adriano's outstanding interest in recent years has been an understanding of color confinement in QCD.¹ His particular sense of beauty in physics has brought to the field the idea that confinement can be understood in terms of a symmetry.² The role of magnetic monopoles can then be exposed by constructing a disorder parameter that tests the magnetic properties of the vacuum.³ Many of the concepts can be exported to other theories where dual excitations are conjectured to play a role in determining the phase structure of the system; compact abelian lattice gauge theory in 3 dimensions is one such theory. This model, which we will refer to as "quenched compact QED₃", has been understood for many years as a field theory example where interesting IR effects such as linear charge confinement and generation of a mass gap arise as an effect of monopoles^{4,5,6} (which in 3d are not particles but *instantons*). As the continuum limit is approached the system remains in the confining phase found at strong coupling, with the vacuum thought of as a dilute charge-neutral plasma of monopoles m and antimonopoles \bar{m} whose effect is to Debye-screen the Coulomb potential of a test charge. The photon mass is proportional to $\exp(-C/e^2)$, e being the electric charge appearing in the relation between gauge potential and link variables $U_{\mu x} = \exp(iaeA_{\mu x})$, where a is the lattice spacing and $C(a)$ related to the free energy of an isolated Dirac monopole. Although this scale is $O(a^{-1})$ implying that the monopole has a core extending over a few lattice spacings where UV artifacts are significant, following Polyakov's original treatment⁴ the model can be viewed as an effective description of the Higgs phase of a 3d Georgi-Glashow model in which semi-classical solutions exist for m and \bar{m} , and hence a continuum limit identified as $\beta \equiv 1/e^2 a \rightarrow \infty$.

More recently people have begun to ask if this situation persists if light electrically-charged fermions are present, in which case the model is now “compact QED₃”. A simple way of seeing why this might be expected to have a dramatic effect is to observe that as a result of the Dirac quantisation condition the combination eg , where g is the magnetic charge of the monopole, is a renormalisation group invariant,⁷ implying $g_R > g$. Hence, virtual electron anti-electron pairs anti-screen the $m\bar{m}$ interaction. More detailed calculations^{8,9} suggest that $V_{m\bar{m}}(x)$ is modified from the 3d Coulomb form $1/x$ to $\ln x$, implying that a deconfined phase with monopoles only present within tightly-bound $m\bar{m}$ molecules, and therefore unable to influence the IR physics, may exist for sufficiently large β . Other workers, however, have argued that interaction among magnetic dipole pairs restores the Coulomb potential at large x , and that confinement continues to survive the continuum limit.¹⁰

A related question is whether there exists a chiral symmetry restoring transition at some finite β_c (like confinement, spontaneous chiral symmetry breaking leading to a mass gap for fermion excitations is known to happen at strong coupling¹¹). In *non-compact* QED₃ in which the Wilson action is replaced by a simple $F_{\mu\nu}^2$ term which is a non-periodic function of the plaquette, so that monopoles are suppressed and play no role in the continuum limit, this issue is believed to depend sensitively on the number of fermion species N_f . Chiral symmetry breaking is supposed to persist in the continuum limit for $N_f < N_{fc}$, where the critical value N_{fc} has been estimated as anything between $\frac{3}{2}$ and ∞ ,^{12,13} with recent estimates based on truncated Schwinger-Dyson equations yielding $N_{fc} \approx 4$.¹⁴ Lattice estimates have proved inconclusive due to the enormous separation of scales predicted by the SD approach (eg. the combination $\langle \bar{\psi}\psi \rangle / e^2 \sim O(10^{-4} - 10^{-5})$): so far studies on lattices up to 80^3 suggest $N_{fc} > 1$.¹⁵

It is intriguing that in QED₃ the two classic non-perturbative phenomena are accounted for by very different theoretical approaches; confinement is attributed to instanton effects whereas chiral symmetry breaking is accounted for by self-consistent solution of the SD equations. An interesting issue raised by these considerations is whether compact and non-compact models have the same continuum limit, which seems probable if indeed monopoles are irrelevant for IR physics. Are any other continuum scenarios possible beyond a confining gapped theory and a deconfined chirally symmetric one? How in fact is “confinement” characterised in the presence of dynamical electric charges? How does everything depend on the parameter N_f ? These questions may have important potential applications in condensed matter physics,^{8,9,10} and have stimulated recent numerical work.^{16,17}

2 The Lattice Model

In this paper we will present the results of numerical simulations of a variant of compact lattice QED₃ in which an extra four-fermion contact term has been added to the action, which in terms of real-valued link potentials $\theta_{\mu x}$ and $N_f/2$ -component staggered fermion fields $\psi_x, \bar{\psi}_x$ reads

$$S = \sum_{xy} \bar{\psi}_x (D_{xy} + M_{xy}) \psi_y + \frac{\beta_s}{2} \sum_x \sigma_x^2 + \beta \sum_{x,\mu<\nu} (1 - \cos \Theta_{\mu\nu x}) \quad (1)$$

where $D_{xy} = \frac{1}{2} \sum_{\mu} \eta_{\mu x} (e^{i\theta_{\mu x}} \delta_{y, x+\hat{\mu}} - e^{-i\theta_{\mu x}} \delta_{y, x-\hat{\mu}})$, $M_{xy} = (\mathcal{M} + \frac{1}{8} \sum_{\langle \tilde{x}, x \rangle} \sigma_{\tilde{x}}) \delta_{xy}$, and $\Theta_{\mu\nu x} = \Delta_{\mu}^{+} \theta_{\nu x} - \Delta_{\nu}^{+} \theta_{\mu x}$. Here $\eta_{\mu x}$ are Kawamoto-Smit phases, σ a real-valued scalar auxiliary field defined on the dual lattice sites \tilde{x} , and $\langle \tilde{x}, x \rangle$ denotes the set of 8 dual sites neighbouring x . Gaussian integration over σ yields an attractive four-fermion interaction of the form $-G(\bar{\psi}\psi)^2$, with the coupling $G \propto 1/\sqrt{\beta_s}$. Pure compact lattice QED₃ is recovered in the limit $\beta_s \rightarrow \infty$.

The four-fermi term has been introduced in studies of $4d$ models¹⁸ to enable simulations in the massless limit $\mathcal{M} = 0$. Although in the limit $\beta \rightarrow \infty$ it induces chiral symmetry breaking in its own right for some $\beta_s < \beta_{sc}$, in $4d$ the extra interaction is irrelevant, and should leave the continuum limit unaltered as β_s is made large. In $3d$ the situation is less clear: $\beta_{sc} \approx 0.25N_f$ defines a UV-stable renormalisation group fixed point,¹⁹ so that while we may suppose that as β_s/β is increased any non-perturbative behaviour such as chiral symmetry breaking may be attributed to gauge dynamics such as monopoles, it remains to be checked that this behaviour is not simply associated with the fixed point of the $3d$ Gross-Neveu model. Note also that the four-fermi term reduces the chiral symmetry group from $U(1)$ to Z_2 .

Magnetic monopoles in the lattice model (1) are identified *à la* DeGrand-Toussaint²⁰ for every plaquette the Dirac string content is identified via

$$\Theta_{\mu\nu x} = \bar{\Theta}_{\mu\nu x} + 2\pi s_{\mu\nu x} \quad (2)$$

where $\bar{\Theta} \in (-\pi, \pi]$ and s is integer. Gauge invariant integer magnetic charges on the dual sites are then given by

$$\tilde{m}_{\tilde{x}} = \epsilon_{\mu\nu\lambda} \Delta_{\mu}^{+} s_{\nu\lambda x}. \quad (3)$$

Since on a 3-torus the total magnetic charge $\sum_x \tilde{m}_{\tilde{x}} \equiv 0$, we find it useful to define the average magnetic charge magnitude per site $m = V^{-1} \sum_x |\tilde{m}_{\tilde{x}}|$ as a measure of monopole activity.

We have performed simulations with $N_f = 4$, $\mathcal{M} = 0$, using a hybrid molecular dynamics algorithm. Fig. 1 sets the scene. We show both $\Sigma \equiv \langle \sigma \rangle = \beta_s^{-1} \langle \bar{\psi}\psi \rangle$, and $\langle m \rangle$ as functions of β , for two four-fermi couplings $\beta_s = 2.0$ and $\beta_s = 4.0$. Broadly speaking we see that chiral symmetry breaking is approximately restored at large β , the transition occurring at a coupling $\beta_c(\beta_s)$ which grows stronger as β_s is increased. There are corresponding peaks in the scalar susceptibility at the same locations (see Fig. 4 below), suggesting that a true phase transition occurs. There is not yet enough data on different volumes to make a definitive statement about the nature or order of this transition; since it has proved so difficult to identify N_{fc} from simulations on finite systems,¹⁵ we should not exclude the possibility of a first order transition to a high- β phase where chiral symmetry is still very slightly broken. What we can say, though, is that the fermions in the weakly coupled phase $\beta > \beta_c$ are much lighter. We also see that $\langle m \rangle$ decreases monotonically with β , with both $\langle \bar{\psi}\psi \rangle$ and $\langle m \rangle$ becoming ‘‘small’’ at $\beta \approx 1.5$ for $\beta_s = 2.0$. This correlation between chiral condensate and magnetic charge density was first observed by Fiebig and Woloshyn,²¹ and more recently by Fiore *et al.*¹⁶ The correlation looks less convincing, however, for $\beta_s = 4.0$, since changing β_s has relatively little effect on $\langle m \rangle$.

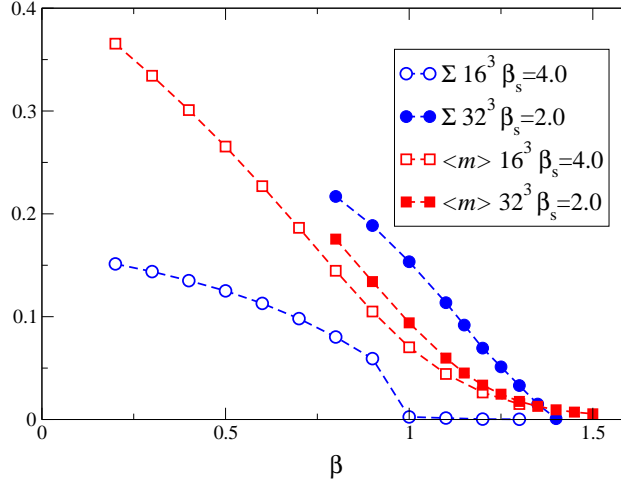


Figure 1: Scalar condensate Σ and magnetic charge density $\langle m \rangle$ vs. β for two values of β_s

3 A Fresh Approach

As Adriano once memorably reminded us, ascribing properties such as confinement to a system because of the presence of monopoles is a little like claiming a metal is superconducting simply because it contains electrons. A more sophisticated characterisation of the vacuum is needed. Unfortunately, here it is impossible to construct a disorder parameter signalling a broken symmetry associated with monopole condensation, as in $4d$ abelian lattice gauge theory,²² because as mentioned above in $3d$ monopoles are not particles. Instead, we will follow an approach introduced in studies of $3d$ non-abelian gauge theories,²³ and look at the difference in free energy and its derivatives, and in particular their dependence on lattice volume, when a magnetic test charge is introduced. Physically this is akin to probing the properties of the resulting magnetic field in the presence of both dynamical monopoles and dynamical electrons: is it screened, indicating persistence of confinement, or can its effects operate over arbitrarily large distances?

First let us review the construction, beginning with the quenched case. The free energy of the system is implicitly given by

$$Z = e^{-\beta F} = \int \mathcal{D}\theta_\mu e^{-S}, \quad (4)$$

with as usual

$$S = \beta \sum_{x,\nu>\mu} (1 - \cos \Theta_{\mu\nu x}). \quad (5)$$

Assuming that the action in the magnetic charge $q \neq 0$ sector has the same form, we can rewrite the same expressions for a system in the presence of an external monopole:

$$Z_M = e^{-\beta F_M} = \int \mathcal{D}\theta_\mu e^{-S_M}, \quad (6)$$

$$S_M = \beta \sum_{x, \nu > \mu} \left(1 - \cos \tilde{\Theta}_{\mu\nu x} \right). \quad (7)$$

with $\tilde{\Theta}_{\mu\nu}$ defined below. The difference in free energy we are looking for is then formally

$$\Delta F = F_M - F = \frac{1}{\beta} \log \frac{Z}{Z_M}. \quad (8)$$

Because of the difficulty in measuring partition functions in lattice simulations, we define²⁴

$$\rho = \frac{\partial}{\partial \beta} (\beta \Delta F) = \langle S_M \rangle_{S_M} - \langle S \rangle_S. \quad (9)$$

The subscript indicates the action with respect to which the average is taken. To determine $\langle S_M \rangle_{S_M}$ an independent simulation using the action S_M instead of S is needed, implying a duplication of computational effort. By integrating ρ we could in principle determine ΔF . However, unless we are interested in its precise value, the general features of the physics can be extracted directly from ρ : eg. we might expect it to display a sharp peak in the critical region if monopoles have something to do with any phase transition. We can also monitor other observables, such as $\Delta m \equiv \langle m \rangle_{S_M} - \langle m \rangle_S$, $\Delta \langle \bar{\psi} \psi \rangle$, etc.

For the form of the action (7), a naive proposal is to use the expression

$$\tilde{\Theta}_{\mu\nu x} = \Theta_{\mu\nu x} + B_{\mu\nu x}, \quad \mu, \nu = 1, 2, 3, \quad (10)$$

where $B_{\mu\nu x} = \Delta_\mu^+ b_{\nu x} - \Delta_\nu^+ b_{\mu x}$ is the plaquette built with the link field

$$\vec{b}(\vec{r}) = \frac{q}{2} \frac{\vec{r} \times \hat{n}}{r(r - \vec{r} \cdot \hat{n})}, \quad (11)$$

which is the vector potential of a Dirac monopole located at $\vec{r} = \vec{0}$ carrying q units of magnetic charge with string along \hat{n} . The action in this form would have nice properties, like the correct continuum limit and invariance under gauge transformations on the field \vec{b} . However, if we adopt this form, we cannot use periodic boundary conditions. In fact, it is easy to see that a simple link shift $\theta_{\mu x} \mapsto \theta_{\mu x} + b_{\mu x}$ will reabsorb \vec{b} into the partition function, so $Z_M = Z$ and no information on ΔF can be extracted.

Our proposal is to keep standard boundary conditions for all dynamical fields, but to use free boundary conditions on the magnetic field. In other words, the lattice topology seen by \vec{b} is not that of an hypertorus, but that of a standard cube. This ensures a net magnetic flux exiting the box, and hence by Gauss's law a non-zero magnetic charge. This "mixed topology" requires extra care for the plaquettes on the bottom face (i.e. with a coordinate equal to 0) of the lattice: since we have to take account also of the contribution of the external field on the top face, these plaquettes enter the action twice, with different $B_{\mu\nu}$. The action then reads

$$\begin{aligned} S_M / \beta &= \sum_{P \in \mathcal{B}} \left(1 - \frac{1}{2} \cos(\Theta_{\mu\nu} + B_{\mu\nu}^{up}) - \frac{1}{2} \cos(\Theta_{\mu\nu} + B_{\mu\nu}^{down}) \right) \\ &+ \sum_{P \notin \mathcal{B}} (1 - \cos(\Theta_{\mu\nu} + B_{\mu\nu})) , \end{aligned} \quad (12)$$

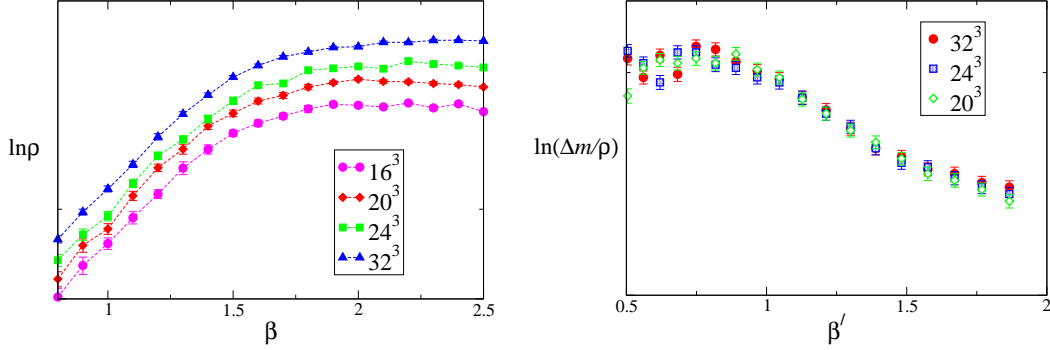


Figure 2: Quenched results: (left) $\ln \rho$ and (right) $\ln(\Delta m / \rho)$ vs. β for various lattice sizes.

where P is the generic plaquette, \mathcal{B} is the boundary of the lattice and the superscripts *up* and *down* refer respectively to the top and bottom faces of the lattice.

When fermions are introduced, the interaction with the the external field entails the following replacements in D_{xy} :

$$e^{i\theta_{\mu x}} \rightarrow e^{i(\theta_{\mu x} + b_{\mu x})} = e^{i\theta_{\mu x}} \zeta_{\mu x}. \quad (13)$$

With \mathcal{B}' the boundary without the edges, \mathcal{E} the edges and \mathcal{M} the bulk without the boundary, and denoting a generic link by $\ell \equiv (x, \mu)$ we have:

$$\zeta_{\ell} = \begin{cases} e^{ib_{\mu x}^{up}} & \ell \in \mathcal{M} \\ \frac{1}{2} \left(e^{ib_{\mu x}^{up}} + e^{ib_{\mu x}^{down}} \right) & \ell \in \mathcal{B}' \\ \frac{1}{4} \left(e^{ib_{\mu x}^{up1}} + e^{ib_{\mu x}^{up2}} + e^{ib_{\mu x}^{up12}} + e^{ib_{\mu x}^{down}} \right) & \ell \in \mathcal{E} \end{cases} \quad (14)$$

A link in the edge must be identified with three other parallel links, here called *up1*, *up2* and *up12*. Note that the ζ couplings on the boundary are not unitary.

4 The Quenched Theory

We first illustrate these ideas in the quenched model, where we “know” the answer. The left panel of Fig. 2 presents $\ln \rho(\beta)$ for lattices ranging from 16^3 up to 32^3 , and shows a crossover from strong to weak coupling behaviour at $\beta \approx 1.5$, whose location is volume independent. The behaviour at weak coupling can be accounted for by Polyakov’s model of the QED_3 vacuum as a dilute neutral monopole plasma. The screened Coulomb potential is

$$V(r) \propto \frac{e^{-Mr}}{r} \quad (15)$$

with⁴

$$M^2 = 4\pi^2 \beta \exp(-\beta C) \equiv 4\pi^2 \beta \xi \quad (16)$$

where ξ is the monopole fugacity. We can use this effective potential to estimate the excess action in the presence of a test magnetic charge. The Lagrangian density $\mathcal{L} \propto H^2(r)$, with $\vec{H} \propto -\vec{\nabla}V$. Therefore

$$\rho = \int d^3r \mathcal{L}(r) \propto 4\pi \int_a^L dr e^{-2Mr} \left[M + \frac{1}{r} \right]^2. \quad (17)$$

The UV contribution dominates the integral; since $Ma \sim \exp(-C\beta)$ we deduce that at weak coupling

$$\rho \sim \frac{4\pi}{a} e^{-2Ma} \propto \exp(-4\pi\sqrt{\beta}e^{-C\beta/2}), \quad (18)$$

and thus that ρ depends only weakly on β in the continuum limit. The data of Fig. 2 support this, with the proviso that even on 32^3 there is no sign of the saturation as $L \rightarrow \infty$ predicted by (17).

With a few more assumptions it is possible to estimate Δm . The density of m (\bar{m}) is proportional to $\xi e^{\pm gV(r)}$, where $g = 2\pi\sqrt{\beta}$ is given by Dirac quantisation. With the (surely too crude) approximation that m and \bar{m} densities are uncorrelated we can write

$$\Delta m \propto \xi \int d^3r [\cosh(2\pi\sqrt{\beta}V(r)) - 1]. \quad (19)$$

For large r the integrand may be approximated as $2\pi^2\beta V^2$, so

$$\Delta m \propto \sqrt{\beta} e^{-C\beta/2} \exp(-4\pi\sqrt{\beta}e^{-C\beta/2}) \Rightarrow \frac{\Delta m}{\rho} \propto \sqrt{\beta} e^{-C\beta/2}. \quad (20)$$

The right panel of Fig. 2 shows that the ratio $\Delta m/\rho$ predicted in (20) is qualitatively correct for $\beta' \gtrsim 1$, and moreover volume independent as $L \rightarrow \infty$, suggesting that the simulation is able to probe the dilute plasma characteristic of the continuum limit. Note that the β -axis has been reparametrised,⁶

$$\beta'(\beta) = \left[2 \ln \left(\frac{I_0(\beta)}{I_1(\beta)} \right) \right]^{-1}, \quad (21)$$

to match the Wilson to the Villain form of the lattice QED₃ action, for which the Polyakov picture should be more accurate. Unfortunately quantitative agreement is less good; our data yield a value for C smaller than the analytic prediction,^{5,25} and the positive curvature at large β is hard to explain, probably requiring a better treatment of $m - \bar{m}$ correlations.

5 Results

We now present results obtained from $O(10^6)$ HMD simulation trajectories of each of the actions (1) and (12,13) on 16^3 , 20^3 and 24^3 lattices, using both $\beta_s = 2.0$ and $\beta_s = 4.0$.

The left panel of Fig. 3 shows $\rho(\beta)$ for the three different volumes at $\beta_s = 2.0$. The curves peak at $\beta \approx 1.3$, with no significant evidence for the position of the peak changing with volume. As in the quenched case, ρ increases with volume and there is

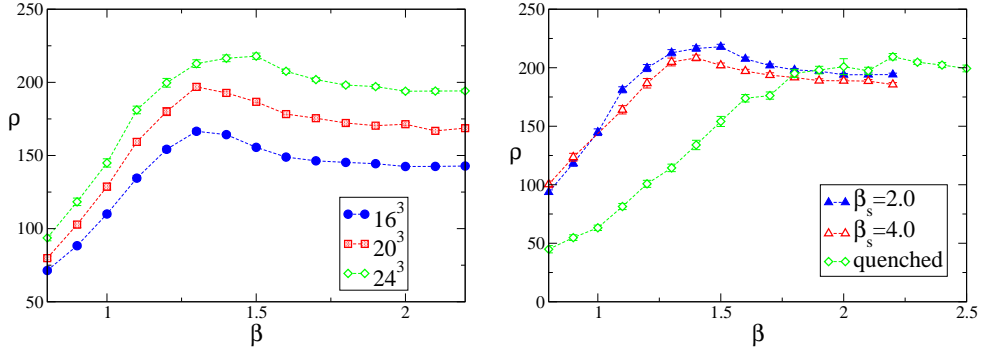


Figure 3: ρ vs. β for $\beta_s = 2.0$ on various lattices (left), and for different β_s on 24^3 (right)

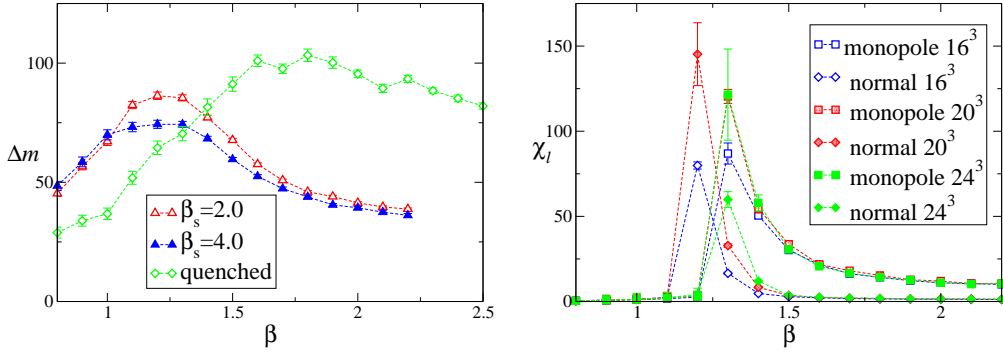


Figure 4: Δm vs. β for various β_s on 24^3 (left), and χ_l vs. β for $q = 0, 1$ on various lattices (right)

no sign of saturation; however, there is also no sign of a divergence, either at a particular β^* , signalling a phase transition, or for a range of values of β , signalling an infinite free energy for the $q \neq 0$ sector and hence a phase in which magnetic charge is confined. In the right hand panel we compare the 24^3 results of the two fermionic models with the corresponding quenched data. There is remarkably little difference between $\beta_s = 2.0$ and $\beta_s = 4.0$; the main effect seems to be a shift of the peak towards stronger coupling compared with quenched, a generic result of electric charge screening due to virtual fermion pairs. The peak location is independent of β_s , unlike the apparent location of the chiral transition β_c seen in Fig. 1. So far there is no reason to interpret the $\rho(\beta)$ data as describing anything other than a crossover from strong to weak coupling, as in the quenched case.

The left hand panel of Fig. 4 tells a similar story for Δm . This quantity probes the cloud of virtual $m\bar{m}$ pairs produced by the plasma to screen the external magnetic charge. Once again there is a well-defined peak, this time at a slightly stronger coupling, and still well to the left of the quenched peak. An interesting feature is that the two fermionic curves only differ significantly in shape in the range $1.0 \lesssim \beta \lesssim 1.4$ – Fig. 1 confirms that in this region the fermions are massive for the $\beta_s = 2.0$ theory but massless (or at least much lighter) for $\beta_s = 4.0$. This suggests that light fermions are able to suppress the

production of virtual $m\bar{m}$ pairs to some extent. There is, however, no evidence that the large- β behaviour differs from the quenched theory.

Finally, the right hand panel of Fig. 4 shows the chiral susceptibility $\chi_l = \partial\langle\bar{\psi}\psi\rangle/\partial\mathcal{M}$ (or at least its disconnected component) versus β , separately in both “normal” $q = 0$ and “monopole” $q = 1$ vacua on the three different volumes. The peaks are consistent with the chiral phase transition at $\beta_c \simeq 1.4$ seen in Fig. 1, but it is interesting that chiral symmetry restoration seems to occur at a slightly weaker coupling in the presence of an external monopole. This can be understood semi-classically; the energy of a spin-singlet $\psi\bar{\psi}$ pair is lowered in the presence of a magnetic field since the constituents have parallel magnetic moments, so pair condensation is promoted. The vacuum therefore contains more $\psi\bar{\psi}$ pairs in the vicinity of the external monopole, and the resulting inhomogeneity in $\langle\bar{\psi}\psi\rangle$ increases χ_l . Fig. 4 shows, however, that at least at large β there is no significant increase of this effect with volume, suggesting that the spatial region over which pair enhancement takes place is finite in extent, implying in turn that the external monopole’s field is still Debye-screened by the $m\bar{m}$ plasma even in the presence of light dynamical fermions.

In summary, the data so far are consistent with the scenario that the monopole plasma survives the introduction of dynamical fermions, even once chiral symmetry is apparently restored. We have identified a region of crossover from strong to weak-coupling behaviour similar in nature to that seen in the quenched theory, and there is no sign of any phase transition or singular free energy in the magnetic sector. Moreover there is no obvious relation between the chiral transition and the crossover. At this stage, therefore, we favour the scenario of Ref. 10 over that of Ref. 9, with all the usual caveats about the need for a more quantitative data analysis, better data in the critical regions, and better understanding of the volume scaling. . .

While we have at least a provisional answer to the question of monopole survival, the nature of the continuum limit of compact QED₃ remains intriguing. Is chiral symmetry truly restored, at least for $N_f \geq 4$? If so, we have an example of a theory which is both “confining” and chirally symmetric! Perhaps this can be understood in the sense of a finite-ranged interaction between conserved fermion currents; we can speculate whether the continuum limit coincides with those of the $\chi U\phi_3$ fermion-gauge-scalar model,²⁶ or even the 3d Thirring model²⁷ at their UV fixed points. An alternative scenario¹⁰ is that chiral symmetry remains broken in the continuum limit, but at a scale far too small to be detected on currently available lattices. In this case the distinction between compact and non-compact theories persists as the issue of whether the photon is gapped or not. What is clear is that QED₃, apparently the simplest of gauge theory models, continues to tantalise us even after more than 15 years of numerical study.

Acknowledgments

SJH was supported in part by a PPARC Senior Research Fellowship, JBK by NSF grant PHY 03-04252, and BL by a Royal Society University Research Fellowship. The bulk of the simulations were performed on a dual-opteron Beowulf cluster at ETH Zürich.

References

1. A. Di Giacomo, *Acta Phys. Polon.* **B36**, 3723 (2005).
2. A. Di Giacomo, *Acta Phys. Polon.* **B25**, 215 (1994).

3. A. Di Giacomo, B. Lucini, L. Montesi and G. Paffuti, *Phys. Rev.* **D61**, 034504 (2000).
4. A.M. Polyakov, *Nucl. Phys.* **B120**, 429 (1977); *Gauge Fields and Strings*, pp. 65-68 (Harwood, 1987).
5. T. Banks, R. Myerson and J.B. Kogut, *Nucl. Phys.* **B129**, 493 (1977).
6. R.J. Wensley and J.D. Stack, *Phys. Rev. Lett.* **63**, 1764 (1989).
7. G. Calucci and R. Jengo, *Nucl. Phys.* **B223**, 501 (1983).
8. J.B. Marston, *Phys. Rev. Lett.* **64**, 1166 (1990).
9. H. Kleinert, F.S. Nogueira and A. Sudbø, *Phys. Rev. Lett.* **88**, 232001 (2002); *Nucl. Phys.* **B666**, 361 (2003).
10. I.F. Herbut and B.H. Seradjeh, *Phys. Rev. Lett.* **91**, 171601 (2003); M.J. Case, B.H. Seradjeh and I.F. Herbut, *Nucl. Phys.* **B676**, 572 (2004).
11. M. Salmhofer and E. Seiler, *Commun. Math. Phys.* **139**, 395 (1991) [Erratum-ibid. **146**, 637 (1992)].
12. T. Appelquist, A.G. Cohen and M. Schmaltz, *Phys. Rev.* **D60**, 045003 (1999).
13. M.R. Pennington and S.R. Webb, Brookhaven preprint BNL-40886; M.R. Pennington and D. Walsh, *Phys. Lett.* **B253**, 246 (1991).
14. P. Maris, *Phys. Rev.* **D54**, 4049 (1996).
15. S.J. Hands, J.B. Kogut and C.G. Strouthos, *Nucl. Phys.* **B645**, 321 (2002); S.J. Hands, J.B. Kogut, L. Scorzato and C.G. Strouthos, *Phys. Rev.* **B70**, 104501 (2004).
16. R. Fiore, P. Giudice, D. Giuliano, D. Marmottini, A. Papa and P. Sodano, *Phys. Rev.* **D72**, 094508 (2005) [Erratum-ibid. **D72**, 119902 (2005)].
17. G. Arakawa, I. Ichinose, T. Matsui and K. Sakakibara, *Phys. Rev. Lett.* **94**, 211601 (2005).
18. S. Kim, J.B. Kogut and M.P. Lombardo, *Phys. Lett.* **B502**, 345 (2001).
19. S.J. Hands, A. Kocić and J.B. Kogut, *Ann. Phys. (N.Y.)* **224**, 29 (1993).
20. T.A. DeGrand and D. Toussaint, *Phys. Rev.* **D22**, 2478 (1980).
21. H.R. Fiebig and R.M. Woloshyn, *Phys. Rev.* **D42**, 3520 (1990).
22. J. Frölich and P.A. Marchetti, *Commun. Math. Phys.* **112**, 343 (1987); L. Polley and U.-J. Wiese, *Nucl. Phys.* **B356**, 629 (1991); A. Di Giacomo and G. Paffuti, *Phys. Rev.* **D56**, 6816 (1997).
23. A. Hart, B. Lucini, Z. Schram and M. Teper, *JHEP* **0006**, 040 (2000); A.C. Davis, A. Hart, T.W.B. Kibble and A. Rajantie, *Phys. Rev.* **D65**, 125008 (2002).
24. L. Del Debbio, A. Di Giacomo and G. Paffuti, *Phys. Lett.* **B349**, 513 (1995).
25. J. Ambjørn, A.J.G. Hey and S. Otto, *Nucl. Phys.* **B210** [FS6], 347 (1982).
26. I.M. Barbour, N. Psycharis, E. Focht, W. Franzki and J. Jersák, *Phys. Rev.* **D58**, 074507 (1998).
27. S.J. Hands and B. Lucini, *Phys. Lett.* **B461**, 263 (1999).